Mathematics in Applied Sciences and Engineering
Volume **5**, Number **4**, December **2024**, pp.**343-367**
https://ojs.lib.uwo.ca/mase
https://doi.org/10.5206/mase/20176

COMPACT SCHEME WITH TWO-SIDED ESTIMATES FOR NONLINEAR CONVECTION-DIFFUSION-REACTION EQUATIONS

CHINEDU NWAIGWE

Dedicated to the memory of Late Professor Mark Rodger, the former Director of the Centre for Scientific Computing, University of Warwick, UK.

Abstract. It is desirable that a numerical method is high-order accurate, compact, efficient and able to simulate purely convection problems. Most existing high-order methods for convection-diffusion-reaction equations (CDREs) either cannot simulate purely-convection problems, or reduce to first order when they can, or require larger stencil to maintain high-order accuracy. This is challenging, especially due to the convection term which can easily lead to oscillatory solutions if naively approximated. This paper proposes a spatially second-order scheme which is able to simulate purely-convection problems with high-order accuracy on minimal stencil. Our idea is based on non-standard central discretization of the convection term. We first discretize the diffusion term in both space and time but discretize the convection term in space only. Next, the semi-discrete convection term is split into positive and negative parts. Transport coefficients are evaluated explicitly in time while different spatial operators are discretized either implicitly or explicitly such that positivity of canonical form is guaranteed. This led to a second-order scheme with all the above desirable properties. Under smoothness assumptions consistency is proved, discrete maximum principle is used to derived two-sided bounds on the numerical solution, and convergence is proved in maximum norm. Several numerical examples are provided to verify the second-order spatial accuracy, convergence and the ability to simulate purely convection problems.

1. Introduction

Consider a region Ω in space occupied by a medium moving with velocity q and having a property, u, which can be concentration, temperature or any other measurable quantity. For instance, u may be the amount (mass concentration) of a pollutant in a river (the moving medium). A practical problem is to determine the time evolution of the quantity u, given its initial distribution in space. Mathematically, this type of problem leads to convection-diffusion equations. Let β represent the diffusivity (diffusion coefficient if u is mass concentration, or thermal conductivity if u is temperature) of u in the medium, s represent the rate of generation/depletion of u through any chemical reaction within the system, and f is the externally generated amount of u that is being added/removed from the medium over time. Assuming that the velocity, q of the moving medium, the diffusivity β, the reaction term, s and the externally generated sources, f of u can be modeled maybe through experiments or other means, then the problem of finding the time evolution of u, given the initial distribution in the medium, can be mathematically stated as follows. Let $x \in (0,1) = \Omega \subset \mathbb{R},\ t \in \mathbb{R}^+$, $q, s : \mathbb{R} \times \Omega \times \mathbb{R}^+ \to \mathbb{R}$, $\beta(u,x,t) \geq 0$

Received by the editors 4 August 2024; accepted 18 November 2024; published online 15 December 2024.
2020 *Mathematics Subject Classification.* 65M06, 65M15.
Key words and phrases. Convection-diffusion equations, nonlinear coefficients, two-sided bounds, experimental order of convergence, consistency, freezing coefficients.

for all u, x, t, and $f : \mathbb{R} \times \mathbb{R}^+ \to \mathbb{R}$: find $u : \Omega \times \mathbb{R}^+ \to \mathbb{R}$ such that:

$$\frac{\partial u}{\partial t} = q(u,x,t)\frac{\partial u}{\partial x} + \frac{\partial}{\partial x}\left(\beta(u,x,t)\frac{\partial u}{\partial x}\right) + s(u,x,t) + f(x,t), \quad \text{for all} \quad (x,t) \in \Omega \times \mathbb{R}^+, \tag{1.1}$$

subject to

$$u(0,t) = \mu_0(t), \quad u(1,t) = \mu_1(t), \ \forall t \geq 0, \tag{1.2}$$

$$u(x,0) = u^0(x) \ \forall x \in \bar{\Omega}. \tag{1.3}$$

The problem (1.1)-(1.3) is called the convection-diffusion-reaction problem. These models appear in the study of many physical and technological applications. In thermal engineering, they model the fluctuations of temperature in moving media with heat sources and sinks, such as in heat exchangers. In environmental engineering, they predict the concentration and transport of pollutants in air, water or soil [15, 28]. In reservoir engineering, they are used to predict oil/water saturation during oil recovery. Similarly, they model the price of option in financial engineering [7, 16, 14, 10]. The theoretical investigation of these equations can be found in [4], see also [41]. It is in one dimension, and with Dirichlet boundary conditions; the two-dimensional extension is left for a different investigation. For existence of unique solution of this problem, we impose the following assumptions [4]: q, β, s, f and their derivatives are uniformly bounded in $C^\infty(\mathbb{R} \times \Omega \times \mathbb{R}^+)$ and

$$\inf_{u,x,t} \beta(u,x,t) > 0. \tag{1.4}$$

For realistic applications, like those involving variable thermal conductivity or variable fluid viscosity, these equations are nonlinear - having nonlinear coefficients such that exact analytical solutions are not known. To this end, numerical approaches are actively being investigated for nonlinear convection-diffusion-reaction (CDR) models, see [12] for example. Hutomo et al [13] investigated a Du-Fort Frankel finite difference algorithm for the 2D CDR problem with variable coefficient. The method was applied to regular and irregular domains, but the model coefficients are linear. A compact scheme, which is fourth-order accurate in time and sixth order in space, is proposed for constant coefficient CDR model in [9]; another compact scheme ultilizing Pade-approximation is also presented in [24].

CDR problems with nonlinear transport properties and coefficients are challenging to approximate, especially due to the convection term. For problems without convection, there are some standard and nonstandard schemes for the diffusion-reaction terms, for example see [6, 25, 30, 34, 33, 31, 20]. When convection is present the problem is more challenging and can lead to unstable solutions if not carefully handled. In this case standard methods no longer work, especially when high-order accurate solution is desired. High-order methods may produce oscillatory solutions [40]. Recent developments and inventions in high-order methods for non-smooth solutions exist in [36, 35, 42, 2, 37, 17, 43]. A common undesirable property of the above high-order non-smooth methods is their non-compact nature. This means that the numerical stencil includes other grid points in addition to a current grid point and its two nearest neighbors (1D) or four in 2D. Therefore, high-order compact schemes for nonlinear CDR problems are still very much desirable.

A compact scheme for nonlinear coupled Burger's equations is proposed in [5] but the problem has constant diffusion coefficients and linear advection coefficient (as in the standard Burger's model). Recent studies [10, 21, 22, 23, 20] have investigated second-order compact finite difference schemes for nonlinear-coefficient convection-diffusion-reaction models. However, these recent schemes cannot be applied in the case when the diffusion coefficient is zero. In particular, they involve division by the diffusion coefficient. This means that the method has to be changed if the problem happens to be a purely convection problem. It is, therefore, desirable to design a method that is capable of handling zero-diffusion problems, where the discretization of the various terms in the equation are de-coupled and each of them remains second-order accurate. This is the thrust of the present study; we extend the range of the diffusion coefficient as follows:

$$\beta(u, x, t) \geq 0, \tag{1.5}$$

instead of

$$\beta(u, x, t) > 0. \tag{1.6}$$

as studied in [10, 21, 22, 23].

Let us state at this point that we are not oblivious that when diffusion is completely absent, the problem becomes hyperbolic which may lead to discontinuities in finite time even when started with smooth initial conditions [39, 18, 19, 38, 29, 26, 3, 1]; this then necessitates the use of conservative methods [39, 18]. However, since high-order conservative schemes are non compact (expensive) and discontinuities only appear after some time, it is still beneficial to use economical (compact) schemes to compute the solution before discontinuities appear. In fact, the numerical results presented in this work show that the solution remains very accurate even when discontinuity is present. Therefore, an accurate high-order CDR solver, that can also handle purely hyperbolic problems, at least for short-duration simulations, is highly desirable.

Our goal is, therefore, to design a second-order finite difference scheme on minimal stencil for fully nonlinear-coefficient convection-diffusion-reaction equations, which is self adaptable to pure convection problems whilst retaining its order of accuracy. The paper is planned as follows: in section 2, we derive the numerical algorithm, and prove its important properties, such as consistency, boundedness and convergence in section 3. Several numerical experiments are provided and discussed in section 4 demonstrating the competitiveness of the proposed method, and the paper is concluded in section 5.

2. Numerical Approximation of the Model

Let $N_x > 0$ be a positive integer, $h = 1/N_x$, Δt be given, $x_i = ih$ for $0 \leq i \leq N_x$, and $t^n = n\Delta t$ for $n \geq 0$. We seek the approximation $u_i^n \approx u(x_i, t^n)$.

Let

$$q_i^n = q(u_i^n, x_i, t^{n+1}),\ ,\beta_i^n = \beta(u_i^n, x_i, t^{n+1}),\ s_i^n = s(u_i^n, x_i, t^{n+1}),\ f_i^{n+1} = f(x_i, t^{n+1}).$$

and define

$$\begin{aligned} &(q_i^+)^n = \frac{q_i^n + |q_i^n|}{2} \geq 0; \quad (q_i^-)^n = \frac{q_i^n - |q_i^n|}{2} \leq 0; \quad q_{i\pm1/2}^n = \frac{q_i^n + q_{i\pm1}^n}{2}; \\ &\beta_{i\pm1/2}^n = \frac{\beta_i^n + \beta_{i\pm1}^n}{2}; \quad \delta^+ u_i^n = \frac{u_{i+1}^n - u_i^n}{h}, \quad \delta^- u_i^n = \frac{u_i^n - u_{i-1}^n}{h}, \end{aligned} \tag{2.1}$$

and let $S_i = \{i | 1 \leq i \leq N_x - 1\}, S_n = \{n | n > 0\}$ and $S_{in} = S_i \times S_n$.

To derive the scheme, we first denote the following exact quantities:

$$\bar{u}_i^n = u(x_i, t^n), \bar{\beta}_i^n = \beta(\bar{u}_i^n, x_i, t^{n+1}), \bar{\beta}_i^{n+1} = \beta(\bar{u}_i^{n+1}, x_i, t^{n+1})$$

and

$$\bar{q}_i^n = q(\bar{u}_i^n, x_i, t^{n+1}), \bar{q}_i^{n+1} = q(\bar{u}_i^{n+1}, x_i, t^{n+1}).$$

By Taylor series expansion, we have:

$$\begin{aligned}\beta(\bar{u}_i^n, x_i, t^{n+1}) &= \beta(\bar{u}_i^{n+1}, x_i, t^{n+1}) + (\bar{u}_i^n - \bar{u}_i^{n+1})\frac{\partial \beta}{\partial u}\bigg|_{(\bar{u}_i^{n+1}, x_i, t^{n+1})} + O(\Delta t^2) \\ &= \beta(\bar{u}_i^{n+1}, x_i, t^{n+1}) + O(\Delta t). \end{aligned} \tag{2.2}$$

and

$$\begin{aligned}\beta(\bar{u}_{i\pm1}^{n+1}, x_{i\pm1}, t^{n+1}) = &\bigg[\beta(\bar{u}_i^{n+1}, x_i, t^{n+1}) \pm h\frac{\partial \beta}{\partial x} + \frac{h^2}{2}\frac{\partial^2 \beta}{\partial x^2} \pm \frac{h^3}{6}\frac{\partial^3 \beta}{\partial x^3} \\ &+ \frac{h^4}{24}\frac{\partial^4 \beta}{\partial x^4} \pm \frac{h^2}{120}\frac{\partial^5 \beta}{\partial x^5} + O(h^6)\bigg]_{(\bar{u}_i^{n+1}, x_i, t^{n+1})}. \end{aligned} \tag{2.3}$$

Using equation (2.2), we get

$$\frac{\left(\bar{\beta}_i^n + \bar{\beta}_{i+1}^n\right)}{2} = \frac{\left(\bar{\beta}_i^{n+1} + \bar{\beta}_{i+1}^{n+1}\right)}{2} + O(\Delta t). \tag{2.4}$$

Using Taylor's Theorem again, we get

$$\begin{aligned}&\bar{\beta}_{i+1/2}^n \delta^+ \bar{u}_i^{n+1} \\ &= \frac{\left(\bar{\beta}_i^n + \bar{\beta}_{i+1}^n\right)\left(\bar{u}_{i+1}^{n+1} - \bar{u}_i^{n+1}\right)}{2h} \\ &= \frac{\left(\bar{\beta}_i^{n+1} + \bar{\beta}_{i+1}^{n+1}\right)\left(\bar{u}_{i+1}^{n+1} - \bar{u}_i^{n+1}\right)}{2h} + O(\Delta t) \\ &= \frac{1}{2h}\bigg[2\bar{\beta} + h\frac{\partial \beta}{\partial x} + \frac{h^2}{2}\frac{\partial^2 \beta}{\partial x^2} + \frac{h^3}{6}\frac{\partial^3 \beta}{\partial x^3} + \frac{h^4}{24}\frac{\partial^4 \beta}{\partial x^4} + \frac{h^2}{120}\frac{\partial^5 \beta}{\partial x^5} \\ &\quad + O(h^6)\bigg]_{(\bar{u}_i^{n+1}, x_i, t^{n+1})} \times \bigg[h\frac{\partial \beta}{\partial x} + \frac{h^2}{2}\frac{\partial^2 \bar{u}}{\partial x^2} + \frac{h^3}{6}\frac{\partial^3 \bar{u}}{\partial x^3} + \frac{h^4}{24}\frac{\partial^4 \bar{u}}{\partial x^4} \\ &\quad + \frac{h^2}{120}\frac{\partial^5 \bar{u}}{\partial x^5} + O(h^6)\bigg]_{(x_i, t^{n+1})} + O(\Delta t) \\ &= \bigg[\beta\frac{\partial u}{\partial x} \\ &\quad + \frac{h}{2}\frac{\partial}{\partial x}\left(\beta\frac{\partial u}{\partial x}\right) \\ &\quad + \frac{h^2}{2}\left(\frac{\beta}{3}\frac{\partial^3 u}{\partial x^3} + \frac{1}{2}\frac{\partial \beta}{\partial x}\frac{\partial^2 u}{\partial x^2} + \frac{1}{2}\frac{\partial^2 \beta}{\partial x^2}\frac{\partial u}{\partial x}\right) \\ &\quad + \frac{h^3}{2}\left(\frac{\beta}{12}\frac{\partial^4 u}{\partial x^4} + \frac{1}{6}\frac{\partial^3 u}{\partial x^3}\frac{\partial \beta}{\partial x} + \frac{1}{4}\frac{\partial^2 u}{\partial x^2}\frac{\partial^2 \beta}{\partial x^2} + \frac{1}{6}\frac{\partial u}{\partial x}\frac{\partial^3 \beta}{\partial x^3}\right) \\ &\quad + \frac{h^4}{2}\left(\frac{\beta}{60}\frac{\partial^5 u}{\partial x^5} + \frac{1}{24}\frac{\partial^4 u}{\partial x^4}\frac{\partial \beta}{\partial x} + \frac{1}{12}\frac{\partial^3 u}{\partial x^3}\frac{\partial^2 \beta}{\partial x^2} + \frac{1}{12}\frac{\partial^2 u}{\partial x^2}\frac{\partial^3 \beta}{\partial x^3} + \frac{1}{24}\frac{\partial u}{\partial x}\frac{\partial^4 \beta}{\partial x^4}\right)\bigg](x_i, t^{n+1}) \\ &\quad + O(\Delta t + h^5). \end{aligned} \tag{2.5}$$

Equation (2.4) is a Taylor series expansion of the preceeding expression. Using the same principles, we also obtain

$$
\begin{aligned}
&\bar{\beta}^n_{i-1/2}\delta^-\bar{u}^{n+1}_i \\
&= \frac{\left(\bar{\beta}^n_i + \bar{\beta}^n_{i-1}\right)\left(\bar{u}^{n+1}_i - \bar{u}^{n+1}_{i-1}\right)}{2h} \\
&= \frac{\left(\bar{\beta}^{n+1}_i + \bar{\beta}^{n+1}_{i-1}\right)\left(\bar{u}^{n+1}_i - \bar{u}^{n+1}_{i-1}\right)}{2h} + O(\Delta t) \\
&= \Bigg[\beta\frac{\partial u}{\partial x} - \frac{h}{2}\frac{\partial}{\partial x}\left(\beta\frac{\partial u}{\partial x}\right) + \frac{h^2}{2}\left(\frac{\beta}{3}\frac{\partial^3 u}{\partial x^3} + \frac{1}{2}\frac{\partial \beta}{\partial x}\frac{\partial^2 u}{\partial x^2} + \frac{1}{2}\frac{\partial^2 \beta}{\partial x^2}\frac{\partial u}{\partial x}\right) \\
&\quad - \frac{h^3}{2}\left(\frac{\beta}{12}\frac{\partial^4 u}{\partial x^4} + \frac{1}{6}\frac{\partial^3 u}{\partial x^3}\frac{\partial \beta}{\partial x} + \frac{1}{4}\frac{\partial^2 u}{\partial x^2}\frac{\partial^2 \beta}{\partial x^2} + \frac{1}{6}\frac{\partial u}{\partial x}\frac{\partial^3 \beta}{\partial x^3}\right) \\
&\quad + \frac{h^4}{2}\left(\frac{\beta}{60}\frac{\partial^5 u}{\partial x^5} + \frac{1}{24}\frac{\partial^4 u}{\partial x^4}\frac{\partial \beta}{\partial x} + \frac{1}{12}\frac{\partial^3 u}{\partial x^3}\frac{\partial^2 \beta}{\partial x^2} + \frac{1}{12}\frac{\partial^2 u}{\partial x^2}\frac{\partial^3 \beta}{\partial x^3} + \frac{1}{24}\frac{\partial u}{\partial x}\frac{\partial^4 \beta}{\partial x^4}\right)\Bigg](x_i, t^{n+1}) \\
&\quad + O(\Delta t + h^5).
\end{aligned} \tag{2.6}
$$

Similarly, the series expansion of $\bar{q}^n_{i\pm1/2}\delta^{\pm}\bar{u}^{n+1}_i$ are obtained by replacing $\bar{\beta}^n_{i+1/2}$ in (2.5) and $\bar{\beta}^n_{i-1/2}$ in (2.6) with $\bar{q}^n_{i+1/2}$ and $\bar{q}^n_{i-1/2}$ respectively. That is,

$$
\begin{aligned}
&\bar{q}^n_{i+1/2}\delta^+\bar{u}^{n+1}_i \\
&= \frac{(\bar{q}^n_i + \bar{q}^n_{i+1})(\bar{u}^{n+1}_{i+1} - \bar{u}^{n+1}_i)}{2h} \\
&= \Bigg[q\frac{\partial u}{\partial x} + \frac{h}{2}\frac{\partial}{\partial x}\left(q\frac{\partial u}{\partial x}\right) + \frac{h^2}{2}\left(\frac{q}{3}\frac{\partial^3 u}{\partial x^3} + \frac{1}{2}\frac{\partial q}{\partial x}\frac{\partial^2 u}{\partial x^2} + \frac{1}{2}\frac{\partial^2 q}{\partial x^2}\frac{\partial u}{\partial x}\right) \\
&\quad + \frac{h^3}{2}\left(\frac{q}{12}\frac{\partial^4 u}{\partial x^4} + \frac{1}{6}\frac{\partial^3 u}{\partial x^3}\frac{\partial q}{\partial x} + \frac{1}{4}\frac{\partial^2 u}{\partial x^2}\frac{\partial^2 q}{\partial x^2} + \frac{1}{6}\frac{\partial u}{\partial x}\frac{\partial^3 q}{\partial x^3}\right) \\
&\quad + \frac{h^4}{2}\left(\frac{q}{60}\frac{\partial^5 u}{\partial x^5} + \frac{1}{24}\frac{\partial^4 u}{\partial x^4}\frac{\partial q}{\partial x} + \frac{1}{12}\frac{\partial^3 u}{\partial x^3}\frac{\partial^2 q}{\partial x^2} + \frac{1}{12}\frac{\partial^2 u}{\partial x^2}\frac{\partial^3 q}{\partial x^3} + \frac{1}{24}\frac{\partial u}{\partial x}\frac{\partial^4 q}{\partial x^4}\right)\Bigg](x_i, t^{n+1}) \\
&\quad + O(\Delta t + h^5),
\end{aligned} \tag{2.7}
$$

and

$$
\begin{aligned}
&\bar{q}^n_{i-1/2}\delta^-\bar{u}^{n+1}_i \\
&= \frac{(\bar{q}^n_i + \bar{q}^n_{i-1})(\bar{u}^{n+1}_i - \bar{u}^{n+1}_{i-1})}{2h} \\
&= \Bigg[q\frac{\partial u}{\partial x} - \frac{h}{2}\frac{\partial}{\partial x}\left(q\frac{\partial u}{\partial x}\right) + \frac{h^2}{2}\left(\frac{q}{3}\frac{\partial^3 u}{\partial x^3} + \frac{1}{2}\frac{\partial q}{\partial x}\frac{\partial^2 u}{\partial x^2} + \frac{1}{2}\frac{\partial^2 q}{\partial x^2}\frac{\partial u}{\partial x}\right) \\
&\quad - \frac{h^3}{2}\left(\frac{q}{12}\frac{\partial^4 u}{\partial x^4} + \frac{1}{6}\frac{\partial^3 u}{\partial x^3}\frac{\partial q}{\partial x} + \frac{1}{4}\frac{\partial^2 u}{\partial x^2}\frac{\partial^2 q}{\partial x^2} + \frac{1}{6}\frac{\partial u}{\partial x}\frac{\partial^3 q}{\partial x^3}\right) \\
&\quad + \frac{h^4}{2}\left(\frac{q}{60}\frac{\partial^5 u}{\partial x^5} + \frac{1}{24}\frac{\partial^4 u}{\partial x^4}\frac{\partial q}{\partial x} + \frac{1}{12}\frac{\partial^3 u}{\partial x^3}\frac{\partial^2 q}{\partial x^2} + \frac{1}{12}\frac{\partial^2 u}{\partial x^2}\frac{\partial^3 q}{\partial x^3} + \frac{1}{24}\frac{\partial u}{\partial x}\frac{\partial^4 q}{\partial x^4}\right)\Bigg](x_i, t^{n+1}) \\
&\quad + O(\Delta t + h^5).
\end{aligned} \tag{2.8}
$$

Subtracting (2.6) from (2.5) we get

$$
\bar{\beta}^n_{i+1/2}\delta^+\bar{u}^{n+1}_i - \bar{\beta}^n_{i-1/2}\delta^-\bar{u}^{n+1}_i = h\frac{\partial}{\partial x}\left(\bar{\beta}\frac{\partial u}{\partial x}\right)(x_i, t^{n+1}) + O(h^3 + \Delta t), \tag{2.9}
$$

while adding (2.7) and (2.8) gives

$$\bar{q}^n_{i+1/2}\delta^+\bar{u}^{n+1}_i + \bar{q}^n_{i-1/2}\delta^-\bar{u}^{n+1}_i = 2\left(q\frac{\partial u}{\partial x}\right)(x_i, t^{n+1}) + O(h^2 + \Delta t). \tag{2.10}$$

Based on (2.9) and (2.10), we adopt the following fully discrete form of the diffusion term

$$\frac{\partial}{\partial x}\left(\beta\frac{\partial u}{\partial x}\right)\Big|_i^{n+1} \approx \frac{\beta^n_{i+1/2}\delta^+u^{n+1}_i - \beta^n_{i-1/2}\delta^-u^{n+1}_i}{h}, \tag{2.11}$$

while we adopt the spatially discrete (time continuous) form of the convection term:

$$\left(q\frac{\partial u}{\partial x}\right)\Big|(x_i, t) \approx \frac{q_{i+1/2}\delta^+u_i + q_{i-1/2}\delta^-u_i}{2}. \tag{2.12}$$

Note that whereas (2.11) is discrete in both space and time, the convection term (2.12) is only discrete in space but still continuous in time. This is important because a naive time discretization of the convection term would lead to oscillatory and/or unstable method. Instead, we first split the spatial approximation (2.12) into its positive and negative parts using $q^\pm = \frac{q\pm|q|}{2}$, see (2.1), so that $q = q^+ + q^-$. This gives

$$\begin{aligned}\left(q\frac{\partial u}{\partial x}\right)\Big|(x_i, t) &\approx \frac{(q^+_{i+1/2} + q^-_{i+1/2})\delta^+u_i + (q^+_{i-1/2} + q^-_{i-1/2})\delta^-u_i}{2}\\ &= \frac{q^+_{i+1/2}\delta^+u_i + q^-_{i+1/2}\delta^+u_i + q^+_{i-1/2}\delta^-u_i + q^-_{i-1/2}\delta^-u_i}{2}.\end{aligned} \tag{2.13}$$

It is now time to obtain the fully discrete (in both space and time) form of the convection term. To do this, we use coefficient freezing for the velocity coefficients, that is we evaluate $q^\pm_{i\pm1/2}$ explicitly. But each of the operators $\delta^\pm u_i$ is evaluated differently - either explicitly or implicitly. This is to ensure positivity of the numerical coefficients in the canonical form which, in turn, ensures boundedness of the approximated solution. To this end, we propose to use implicit evaluation for the operators in the first and last terms on the right of (2.13), while the operators in the second and third terms are evaluated explicitly. This leads to the following fully discrete convection term:

$$\begin{aligned}\left(q\frac{\partial u}{\partial x}\right)\Big|_i^{n+1} \approx& \frac{1}{2}\Big[(q^+_{i+1/2})^n\delta^+u^{n+1}_i + (q^-_{i+1/2})^n\delta^+u^n_i + (q^+_{i-1/2})^n\delta^-u^n_i\\ &+ (q^-_{i-1/2})^n\delta^-u^{n+1}_i\Big].\end{aligned} \tag{2.14}$$

Hence, using (2.11) and (2.14), then applying time discretization for the unsteady term, we derive the following numerical scheme for problem (1.1): find u^n_i for all $i \in S_{in}$ and $n > 0$, such that

$$\begin{aligned}u^{n+1}_i = u^n_i + \Delta t\Big[&\frac{1}{h}\left(\beta^n_{i+1/2}\delta^+u^{n+1}_i - \beta^n_{i-1/2}\delta^-u^{n+1}_i\right)\\ &+ \frac{1}{2}\left((q^+)^n_{i+1/2}\delta^+u^{n+1}_i + (q^-)^n_{i-1/2}\delta^-u^{n+1}_i\right)\\ &+ \frac{1}{2}\left((q^-)^n_{i+1/2}\delta^+u^n_i + (q^+)^n_{i-1/2}\delta^-u^n_i\right)\\ &+ s(u^n_i, x_i, t^{n+1}) + f^{n+1}_i\Big] \quad \forall (i,n) \in S_{in},\\ u^0_i = u^0(x_i) \quad &\forall \quad i \in S_i \cup \{0, N_x\},\\ u^{n+1}_0 = \mu_0(t^{n+1}), \quad &u^{n+1}_{N_x} = \mu_1(t^{n+1}) \quad \forall \quad n.\end{aligned} \tag{2.15}$$

Observed that the convection coefficient is evaluated at the grid midpoints, $i \pm 1/2$, by averaging just like is done for the diffusion coefficient. They are also split into positive and negative parts which are then appropriately discretized using implicit or explicit time scheme. This approach ensures that the positivity of the canonical numerical coefficients, which are necessary for two-sided boundedness, are maintained. This is a unique feature of the algorithm. We also see that the scheme does not require strictly positive diffusion (β) unlike the scheme in [23] which involves division by β. This allows our scheme to be applicable also to purely convection problems (in the absence of shocks). We will show below that the formulation is second order accurate in space and first order in time.

Comment on Newmann Boundary Condition. The last equation in (2.15) is the discrete version of the Dirichlet boundary condition given in (1.2). It is possible that one of the boundary conditions is replaced with a Newmann-type condition. For example, if the left boundary condition is replaced with:

$$\left.\frac{\partial u}{\partial x}\right|_{(0,t)} = \mu_0(t), \ \forall t \geq 0. \tag{2.16}$$

Then, the first equation in the last line of (2.15) would be replaced with:

$$\frac{u_1^{n+1} - u_{-1}^{n+1}}{2h} = \mu_0(t^{n+1}) \quad \forall \quad n, \tag{2.17}$$

where the point x_{-1} corresponds to a "ghost" point at the left side of x_0. In this case the full scheme (the first part of (2.15)) is also applied at the point x_0.

3. Numerical Analysis of the Proposed Method

In this section, we investigate some important properties of the proposed scheme. In particular, we prove that the proposed difference scheme is consistent with the given differential problem; that its solution is bounded; and finally that the solutions computed on a sequence of grids converge to the exact solution of the differential problem.

3.1. **Accuracy - Consistency Analysis.**

Theorem 3.1 (Consistency). Suppose that $u \in \mathbb{C}^\infty(\Omega \times \mathbb{R}^+)$ is the exact solution of (1.1). Then, the scheme (2.15) is consistent with the model (1.1); it is second order accurate in space and first order accurate in time.

Proof. Let $\bar{u}_i^n \equiv u(x_i, t^n)$ as before, then using (2.9) and (2.10), we have

$$\frac{1}{h}\left(\bar{\beta}_{i+1/2}^n \delta^+ \bar{u}_i^{n+1} - \bar{\beta}_{i-1/2}^n \delta^- \bar{u}_i^{n+1}\right) = \frac{\partial}{\partial x}\left(\beta \frac{\partial u}{\partial x}\right)(x_i, t^{n+1}) + O(\Delta t + h^2), \tag{3.1}$$

and

$$\frac{1}{2}\left(\bar{q}_{i+1/2}^n \delta^+ \bar{u}_i^{n+1} + \bar{q}_{i+1/2}^n \delta^- \bar{u}_i^{n+1}\right) = \left(q \frac{\partial u}{\partial x}\right)(x_i, t^{n+1}) + O(\Delta t + h^2). \tag{3.2}$$

But

$$\begin{aligned}
&\frac{1}{2}\left((\bar{q}^+)_{i+1/2}^n \delta^+ \bar{u}_i^{n+1} + (\bar{q}^-)_{i-1/2}^n \delta^- \bar{u}_i^{n+1}\right) + \frac{1}{2}\left((\bar{q}^-)_{i+1/2}^n \delta^+ \bar{u}_i^{n} + (\bar{q}^+)_{i-1/2}^n \delta^- \bar{u}_i^{n}\right) \\
&= \frac{1}{2}\left(\bar{q}_{i+1/2}^n \delta^+ \bar{u}_i^{n+1} + \bar{q}_{i-1/2}^n \delta^- \bar{u}_i^{n+1}\right) + O(\Delta t) \quad (\text{because } \bar{q} = \bar{q}^+ + \bar{q}^-) \\
&= \left(q \frac{\partial u}{\partial x}\right)(x_i, t^{n+1}) + O(\Delta t + h^2) \quad (\text{from (3.2)}).
\end{aligned}$$

Since,

$$\frac{\bar{u}_i^{n+1} - \bar{u}_i^n}{\Delta t} = \frac{\partial u}{\partial t}(x_i, t^{n+1}) + O(\Delta t) \text{ and } s(u_i^{n+1}, x_i, t^{n+1}) = s(u_i^n, x_i, t^{n+1}) + O(\Delta t).$$

Therefore, the truncation error τ_i^n of the scheme (2.15) becomes:

$$\begin{aligned}
\tau_i^n :=& \frac{\bar{u}_i^{n+1} - \bar{u}_i^n}{\Delta t} - \frac{1}{h}\left(\bar{\beta}_{i+1/2}^n \delta^+ \bar{u}_i^{n+1} - \bar{\beta}_{i-1/2}^n \delta^- \bar{u}_i^{n+1}\right) \\
&- \frac{1}{2}\left((\bar{q}^+)_{i+1/2}^n \delta^+ \bar{u}_i^{n+1} + (\bar{q}^-)_{i-1/2}^n \delta^- \bar{u}_i^{n+1}\right) \\
&- \frac{1}{2}\left((\bar{q}^-)_{i+1/2}^n \delta^+ \bar{u}_i^{n} + (\bar{q}^+)_{i-1/2}^n \delta^- \bar{u}_i^{n}\right) - s(\bar{u}_i^n, x_i, t^{n+1}) - f_i^{n+1} \\
=& \frac{\partial u}{\partial t}(x_i, t^{n+1}) - \frac{\partial}{\partial x}\left(\beta \frac{\partial u}{\partial x}\right)(x_i, t^{n+1}) - \left(q \frac{\partial u}{\partial x}\right)(x_i, t^{n+1}) \\
&- s(u_i^{n+1}, x_i, t^{n+1}) - f(x_i, t^{n+1}) + O(\Delta t + h^2) \\
=& O(\Delta t + h^2).
\end{aligned}$$

□

3.2. **Two Sided Bounds for Approximated Solution.** The essense of this subsection is to prove that the solution computed by our proposed scheme is bounded. That is, if u_i^n is bounded for all i, then u_i^{n+1} is bounded for all i and $n \geq 0$. The canonical form (see also [22, 23, 32]) of the scheme is

$$B_i^n u_i^{n+1} = A_{i,L}^n u_{i-1}^{n+1} + A_{i,R}^n u_{i+1}^{n+1} + u_i^n + P_i^n, \tag{3.3}$$

where

$$\begin{aligned}
A_{i,L}^n &= \left(\frac{\beta_{i-1/2}^n}{h^2} - \frac{(q^-)_{i-1/2}^n}{2h}\right)\Delta t,\ A_{i,R}^n = \left(\frac{\beta_{i+1/2}^n}{h^2} + \frac{(q^+)_{i+1/2}^n}{2h}\right)\Delta t, \\
B_i^n &= 1 + A_{i,L}^n + A_{i,R}^n, \\
P_i^n &= \Delta t\Bigg[\frac{1}{2}\left((q^-)_{i+1/2}^n \delta^+ u_i^n + (q^+)_{i-1/2}^n \delta^- u_i^n\right) \\
&\quad + s(u_i^n, x_i, t^{n+1}) + f_i^{n+1}\Bigg].
\end{aligned} \tag{3.4}$$

Lemma 3.1. In (3.4), the following is true:

$$A_{i,L}^n,\ A_{i,R}^n \geq 0. \tag{3.5}$$

Proof. By (2.1), we have

$$(q^-)_{i\pm1/2}^n \leq 0 \quad \text{and} \quad (q^+)_{i\pm1/2}^n \geq 0.$$

Also, by (1.5), we have $\beta_{i\pm1/2}^n$, as defined in (2.1), are non-negative. Since Δt and h are both non-negative, hence $A_{i,L}^n, A_{i,R}^n$ defined in (3.4) are non-negative. □

We now prove the boundedness of the numerical solution.

Theorem 3.2 (Two Sided Bounds). The numerical solution, u_i^{n+1}, computed with the scheme, (3.3), is bounded below and above as follows:

$$\min_i \left[\frac{u_i^n + P_i^n}{B_i^n - A_{i,L}^n - A_{i,R}^n}\right] \leq u_i^{n+1} \leq \max_i \left[\frac{u_i^n + P_i^n}{B_i^n - A_{i,L}^n - A_{i,R}^n}\right]. \tag{3.6}$$

Proof. Let

$$u_{max}^{n+1} = \max_i\{u_i^{n+1}\},\ \ u_{min}^{n+1} = \min_i\{u_i^{n+1}\}.$$

Then, theres exist $i_{min}, i_{max} \in \{1, 2, \cdots, N_x - 1\}$ such that

$$u_{i_{min}}^{n+1} = u_{min}^{n+1} \text{ and } u_{i_{max}}^{n+1} = u_{max}^{n+1},$$

where the neighbors of i_{min} and i_{max} are respectively $i_{min} \pm 1, i_{max} \pm 1 \in \{1, 2, \cdots, N_x - 1\}$. Therefore, applying the scheme (3.3) to $u_{max}^{n+1} = u_{i_{max}}^{n+1}$, we have

$$\begin{aligned} B_{i_{max}}^n u_{i_{max}}^{n+1} &= A_{i_{max},L}^n u_{i_{max}-1}^{n+1} + A_{i_{max},R}^n u_{i_{max}+1}^{n+1} + u_{i_{max}}^n + P_{i_{max}}^n \\ &\leq A_{i_{max},L}^n u_{i_{max}}^{n+1} + A_{i_{max},R}^n u_{i_{max}}^{n+1} + u_{i_{max}}^n + P_{i_{max}}^n. \end{aligned}$$

The last inequality follows from the fact that $A_{i,L}, A_{i,R} \geq 0$ for all $i \in 1, \cdots, N_x - 1$ (see Lemma 3.1). The inequality gives

$$\left(B_{i_{max}}^n - A_{i_{max},L}^n - A_{i_{max},R}^n\right) u_{i_{max}}^{n+1} \leq u_{i_{max}}^n + P_{i_{max}}^n.$$

Since $B_{i_{max}}^n - A_{i_{max},L}^n - A_{i_{max},R}^n = 1 \geq 0$ (see (3.4)), then we have

$$u_{i_{max}}^{n+1} \leq \frac{u_{i_{max}}^n + P_{i_{max}}^n}{B_{i_{max}}^n - A_{i_{max},L}^n - A_{i_{max},R}^n} \leq \max_i \frac{u_i^n + P_i^n}{B_i^n - A_{i,L}^n - A_{i,R}^n}. \tag{3.7}$$

This proves the right inequality in the theorem.

To prove the first inequality, we also proceed by writing the numerical scheme (3.3) for its minimum solution, $u_{i_{min}}^{n+1}$, namely:

$$\begin{aligned} B_{i_{min}}^n u_{i_{min}}^{n+1} &= A_{i_{min},L}^n u_{i_{min}-1}^{n+1} + A_{i_{min},R}^n u_{i_{min}+1}^{n+1} + u_{i_{min}}^n + P_{i_{min}}^n \\ &\geq A_{i_{min},L}^n u_{i_{min}}^{n+1} + A_{i_{min},R}^n u_{i_{min}}^{n+1} + u_{i_{min}}^n + P_{i_{min}}^n. \end{aligned}$$

This leads to

$$u_{i_{min}}^{n+1} \geq \frac{u_{i_{min}}^n + P_{i_{mmin}}^n}{B_{i_{min}}^n - A_{i_{min},L}^n - A_{i_{min},R}^n} \geq \min_i \frac{u_i^n + P_i^n}{B_i^n - A_{i,L}^n - A_{i,R}^n}. \tag{3.8}$$

Combining (3.9) and (3.8), we have:

$$u_i^{n+1} \leq u_{i_{max}}^{n+1} \leq \max_i \frac{P_i^n}{B_i^n - A_{i,L}^n - A_{i,R}^n},$$

and

$$u_i^{n+1} \geq u_{i_{min}}^{n+1} \geq \min_i \frac{u_i^n + P_i^n}{B_i^n - A_{i,L}^n - A_{i,R}^n}.$$

Hence,

$$\min_i \frac{u_i^n + P_i^n}{B_i^n - A_{i,L}^n - A_{i,R}^n} \leq u_i^{n+1} \leq \max_i \frac{u_i^n + P_i^n}{B_i^n - A_{i,L}^n - A_{i,R}^n}$$

as claimed. This proves that if u^n is bounded, then u^{n+1} is bounded. In particular, if the initial solution u^0, $(n = 0)$ is bounded, then the computed solution u^{n+1} is bounded for all $n \geq 0$. □

3.3. **Convergence Analysis.** Let $\bar{u}_i^n = u(x_i, t^n)$ denote the exact solution of the CDR model (1.1) and u_i^n be the numerical solution computed with the proposed scheme, (3.3). Then, the error is defined as $e_i^n := \bar{u}_i^n - u_i^n$; we also define the error norm $\|e^n\| := \max_i |e_i^n|$ also denoted as E^n. Furthermore, let

$$\bar{A}_{i,L}^n = \left(\frac{\bar{\beta}_{i-1/2}^n}{h^2} - \frac{(\bar{q}^-)_{i-1/2}^n}{2h}\right)\Delta t, \quad \bar{A}_{i,R}^n = \left(\frac{\bar{\beta}_{i+1/2}^n}{h^2} + \frac{(\bar{q}^+)_{i+1/2}^n}{2h}\right)\Delta t, \text{ and } \bar{B}_i^n = 1 + \bar{A}_{i,L}^n + \bar{A}_{i,R}^n.$$

Lemma 3.2. Let

$$\bar{P}_i^n = \Delta t\left[\frac{1}{2}\left((\bar{q}^-)_{i+1/2}^n \delta^+ \bar{u}_i^n + (\bar{q}^+)_{i-1/2}^n \delta^- \bar{u}_i^n\right) + s(\bar{u}_i^n, x_i, t^{n+1}) + f_i^{n+1}\right].$$

Then the difference $\bar{P}_i^n - P_i^n$ satisfies the bound

$$\bar{P}_i^n - P_i^n \leq \Delta t(\hat{P}_i^n E^n + O(E^n)) \tag{3.9}$$

where

$$\hat{P}_i^n = \frac{1}{2h}\max_i\left\{\left[|(q_{i+1/2}^-)^n||e_{i+1}^n/e_i^n - 1| + |(q_{i-1/2}^+)^n||1 - e_{i-1}^n/e_i^n|\right]\right\}, \tag{3.10}$$

and P_i^n is given in (3.3).

Proof. Using first order terms of Taylor series, we have the approximation:

$$\begin{aligned}
\bar{P}_i^n - P_i^n =& \frac{\Delta t}{2h}\Bigg[\left((q^-)_{i+1/2}^n + O(e_{i+1/2}^n)\right)(\bar{u}_{i+1}^n - \bar{u}_i^n) - (q^-)_{i+1/2}^n(u_{i+1}^n - u_i^n) \\
&+ \left((q^+)_{i-1/2}^n + O(e_{i-1/2}^n)\right)(\bar{u}_i^n - \bar{u}_{i-1}^n) - (q^+)_{i-1/2}^n(u_i^n - u_{i-1}^n)\Bigg] \\
&+ s(u_i^n, x_i, t^{n+1}) + O(e_i^n) - s(u_i^n, x_i, t^{n+1}) \\
=& \frac{\Delta t}{2h}\left[(q^-)_{i+1/2}^n(e_{i+1}^n - e_i^n) + (q^+)_{i-1/2}^n(e_i^n - e_{i-1}^n)\right] + O(e_{i-1/2}^n) \\
&+ O(e_i^n) + O(e_{i+1/2}^n) \\
=& \frac{\Delta t}{2h}\left[(q^-)_{i+1/2}^n(e_{i+1}^n/e_i^n - 1) + (q^+)_{i-1/2}^n(1 - e_{i-1}^n/e_i^n)\right]e_i^n \\
&+ O(e_{i-1/2}^n) + O(e_i^n) + O(e_{i+1/2}^n) \\
\leq& \frac{\Delta t}{2h}\max_i\left\{\left[|(q_{i+1/2}^-)^n||e_{i+1}^n/e_i^n - 1| + |(q_{i-1/2}^+)^n||1 - e_{i-1}^n/e_i^n|\right]\right\}E^n \\
&+ \Delta t O(E^n) \\
=& \Delta t\hat{P}_i^n E^n + \Delta t O(E^n)
\end{aligned}$$

□

Theorem 3.3 (Convergence Theorem). The error in the numerical solution computed using the scheme (2.15) or (3.3), satisfies the following inequality:

$$E^{n+1} \leq E^n, \quad \text{as } \Delta t \to 0, \text{ for all } n \geq 0.$$

Proof. The consistency theorem 3.1 implies the exact solution $\bar{u}_i^n$ at grid point x_i and time t^n satisfies the numerical scheme (3.3) as follows:

$$(1 + \bar{A}_{i,L}^n + \bar{A}_{i,R}^n)u_i^{n+1} = \bar{A}_{i,L}^n\bar{u}_{i-1}^{n+1} + \bar{A}_{i,R}^n\bar{u}_{i+1}^{n+1} + \bar{u}_i^n + \bar{P}_i^n + \Delta t\tau_i^n,$$

where $\tau_i = O(\Delta t + h^2)$ is the truncation error.

Taylor series expansion of the coefficients $\bar{A}_{i,L}^n, \bar{A}_{i,R}^n$ about $\bar{u}_{i-1/2}^n$ and $\bar{u}_{i+1/2}^n$, respectively, leads to the following:

$$\begin{aligned}
(1 + A_{i,L}^n + A_{i,R}^n)\bar{u}_i^{n+1} =& A_{i,L}^n\bar{u}_{i-1}^{n+1} + \bar{A}_{i,R}^n\bar{u}_{i+1}^{n+1} + \bar{u}_i^n + \bar{P}_i^n + \Delta t\tau_i^n \\
&+ \Delta t\Big[O(e_{i+1/2}^n) + O(e_{i-1/2}^n)\Big]
\end{aligned} \tag{3.11}$$

The error term (the last term on the right) arises from Taylor series expansion, and the factor Δt is present because $A_{i,L}^n$ and $A_{i,R}^n$ are both multiples of Δt.

Subtracting the scheme (3.3) from (3.11), gives:

$$\begin{aligned}(1 + A^n_{i,L} + A^n_{i,R})e^{n+1}_i =& A^n_{i,L}e^{n+1}_{i-1} + A^n_{i,R}e^{n+1}_{i+1} + e^n_i + \bar{P}^n_i - P^n_i + \Delta t\tau^n_i \\ &+ \Delta t\Big[O(e^n_{i+1/2}) + O(e^n_{i-1/2})\Big]\end{aligned} \tag{3.12}$$

Since the coefficients are positive, we can write

$$\begin{aligned}&(1+A^n_{i,L} + A^n_{i,R})\max_i \Big|e^{n+1}_i\Big| \\ &\le \max_i \Big|(1 + A^n_{i,L} + A^n_{i,R})e^{n+1}_i\Big| \\ &= \max_i \Big|A^n_{i,L}e^{n+1}_{i-1} + A^n_{i,R}e^{n+1}_{i+1} + e^n_i + \bar{P}^n_i - P^n_i + \Delta t\tau^n_i \\ &\qquad + \Delta t\Big[O(e^n_{i+1/2}) + O(e^n_{i-1/2})\Big]\Big| \qquad \text{(by using (3.12))} \\ &\le A^n_{max}\|e^{n+1}\| + A^n_{max}\|e^{n+1}\| + \|e^n\| + \Delta t(\hat{P}^n_i\|e^n\| + O(E^n)) + \Delta t\tau^n_i \\ &\quad + \Delta t\Big[O(e^n_{i+1/2}) + O(e^n_{i-1/2})\Big] \\ &\le A^n_{max}\|e^{n+1}\| + A^n_{max}\|e^{n+1}\| + \|e^n\| \text{ as } \Delta t \to 0,\end{aligned}$$

where $A^n_{max} = \max_i\{A^n_{i,L}, A^n_{i,R}\}$, and use has been made of the inequality in Lemma 3.2.

Hence, we have arrived at the inequality:

$$(1+A^n_{i,L} + A^n_{i,R})\|e^{n+1}\| \le \qquad A^n_{max}\|e^{n+1}\| + A^n_{max}\|e^{n+1}\| + \|e^n\| \text{ for all } i.$$

Taking the maximum of both sides the coefficients on the left become $(1 + A^n_{max} + A^n_{max})$. After simplifications, we obtain the inequality:

$$E^{n+1} := \|e^{n+1}\| \le \|e^n\| =: E^n.$$

□

This completes the analysis of the numerical scheme. Below, we present several numerical test cases to verify the numerical scheme and its theoretical properties.

4. Numerical Results

In this section we present several numerical experiments to demonstrate the accuracy of the proposed scheme. The scheme is implemented in the Author's own C++ code that uses the Eign C++ library [8] for all the relevant linear algebra calculations. In each test case, the error is measured in l_2-norm and the experimental order of convergence (EOC) is also computed. The results from the proposed scheme are also compared with those computed with scheme of Matus and co-workers [22, 23]. In the tables below, $M = N_x + 1$ denote the number of grid points, while the phrases NEW SCHEME and MHV refer to the newly proposed scheme and the scheme of Matus and collaborators [22] respectively. Each example is computed on a sequence of grids. The time step for all simulations is computed as $\Delta t = \frac{h^2}{2}$, where h is the mesh size. The Tables are provided to verify the second order of convergence for the proposed scheme (and also re-confirm the convergence of the MHV solver). In addition, graphical plots of the computed solutions at different times are also provided to further demonstrate the accuracy, convergence and competitiveness of the newly proposed scheme. We also included a Table 8 to verify the time order of convergence of the method.

Problem 1: Nonlinear CDR Model. In this first example, we consider the following problem.

$$\frac{\partial u}{\partial t} = -u\frac{\partial u}{\partial x} + \frac{\partial}{\partial x}\left(e^{-u}\frac{\partial u}{\partial x}\right) + u^3 + f(x,t), \tag{4.1}$$

$$u(0,t) = 1 + e^{-t}, \quad u(1,t) = 1 - e^{-t}, \quad u(x,0) = 1 + cos(\pi x). \tag{4.2}$$

where

$$f = \Bigg(\left(\pi^2 e^{-1-e^{-t}\cos(\pi y)} - 1\right) e^{2t}\cos(\pi y) - \left(e^t + \cos(\pi y)\right)^3 + \pi\left(-e^t + \pi e^{-1-e^{-t}\cos(\pi y)}\sin(\pi y) - \cos(\pi y)\right) e^t \sin(\pi y)\Bigg) e^{-3t} \tag{4.3}$$

The exact solution of this problem is:

$$u(x,t) = 1 + e^{-t}\cos(\pi x).$$

Table 1 details the results of the numerical solution outputted after $t = 0.1$ and $t = 1.0$ for various mesh sizes. We can see that the results agree with the exact solution and the theoretical order of convergence is also verified. Noteworthy is that the solution computed by the proposed method is very accurate as much as those of the MHV solver. Furthermore, the graphical plots of the solution computed on a grid of 51 points and outputted at different times ($t = 1, 2, 5, 10, 50$) are shown in Figure 1. Obviously, the results show that the method remains stable, accurate and convergent at all times.

TABLE 1. Error and Experimental Order of Convergence (EOC) for Problem 1, outputted after $t = 0.1$ and $t = 1.0$.

M	MHV-Error	MHV-EOC	New Scheme-Error	New-Scheme-EOC
Results Outputted after time = 0.1				
4	0.02484470	-	0.025327300	-
8	0.01503970	0.724163	0.007568710	1.74257
16	0.00632822	1.248900	0.002065030	1.87389
32	0.00199133	1.668070	0.000522334	1.98312
64	0.00055954	1.831430	0.000131387	1.99114
128	0.00014790	1.919610	3.28929e-05	1.99798
Results Outputted after time = 1.0				
4	0.17813900	-	0.133597000	-
8	0.11062000	0.687396	0.051697600	1.36972
16	0.04986790	1.149420	0.014019000	1.88271
32	0.01687890	1.562890	0.003585330	1.96721
64	0.00482888	1.805460	0.000902372	1.99031
128	0.00128041	1.915080	0.000226082	1.99687

Problem 2: Nonlinear CDR Model. We consider the following problem.

$$\frac{\partial u}{\partial t} + u\frac{\partial u}{\partial x} = \frac{\partial}{\partial x}\left(e^{-u^2}\frac{\partial u}{\partial x}\right) - ue^{-x^2 t} + f(x,t), \tag{4.4}$$

$$u(0,t) = 1,\ u(1,t) = -1, \quad u(x,0) = \cos(\pi x). \tag{4.5}$$

where

$$f(x,t) = \Bigg(2\pi^2 e^{-2t-e^{-2t}\cos^2(\pi y)}\sin^2(\pi y) - 1 + \pi^2 e^{-e^{-2t}\cos^2(\pi y)} + e^{-ty^2} - \pi e^{-t}\sin(\pi y)\Bigg) e^{-t}\cos(\pi y) \tag{4.6}$$

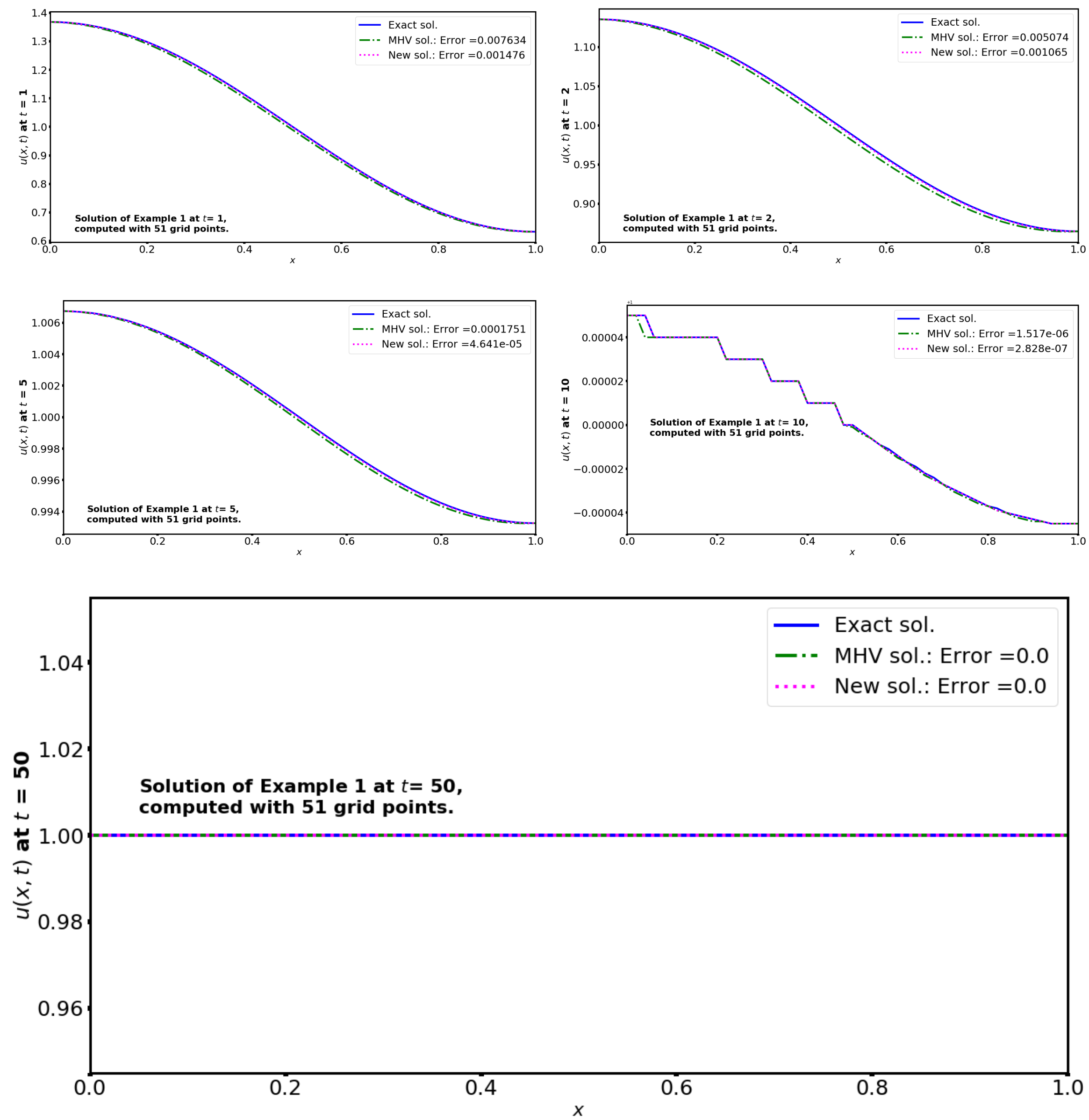

FIGURE 1. Exact and Numerical Solutions of Example 1 computed at different times on a grid of 51 points

The exact solution is

$$u(x,t) = e^{-t}\cos(\pi x).$$

The numerical and exact solutions, for different meshes, are tabulated in Table 2. We can also see that the new scheme is very competitive just like in problem 1. In Figure 2 the exact and numerical solutions are also plotted at different times, and the results also confirm the convergence of the method.

TABLE 2. Numerical Results for Problem 2

M	MHV-Error	MHV-EOC	New Scheme-Error	New-Scheme-EOC
Results Outputted after time = 0.1				
4	0.04422990	-	0.028147100	-
8	0.01235700	1.83970	0.008874660	1.66522
16	0.00299986	2.04236	0.002150850	2.04478
32	0.000742402	2.01462	0.000533402	2.01161
64	0.000185001	2.00467	0.000133063	2.00311
128	4.61998e-05	2.00157	3.32489e-05	2.00073
Results Outputted after time = 1.0				
4	0.00630395	-	0.00466888	-
8	0.00137394	2.19794	0.00103938	2.16736
16	0.000333006	2.0447	0.000252931	2.0389
32	8.26259e-05	2.01088	6.28234e-05	2.00937
64	2.06173e-05	2.00274	1.56806e-05	2.00232
128	5.15182e-06	2.0007	3.91856e-06	2.00058

Problem 3: Nonlinear CDR Model. Again, we consider another nonlinear problem.

$$\frac{\partial u}{\partial t} + u\frac{\partial u}{\partial x} = \frac{\partial}{\partial x}\left(e^{-u}\frac{\partial u}{\partial x}\right) - ue^{-x^2 t} + f(x,t), \tag{4.7}$$

$$u(0,t) = 1,\ u(1,t) = -1, \quad u(x,0) = \cos(\pi x). \tag{4.8}$$

where

$$f(x,t) = \Bigg(\pi^2 e^{-t-e^{-t}\cos(\pi y)}\sin^2(\pi y) - \cos(\pi y) + \pi^2 e^{-e^{-t}\cos(\pi y)}\cos(\pi y) + e^{-ty^2}\cos(\pi y) - \frac{\pi e^{-t}\sin(2\pi y)}{2}\Bigg)e^{-t} \tag{4.9}$$

The exact solution is:

$$u(x,t) = e^{-t}\cos(\pi x).$$

The results outputted after $t = 0.1$ and $t = 1.0$ are tabulated in Table 3, and the numerical results also confirm the accuracy and convergence of the new scheme. Figure 3 shows the plots of the solutions at different times, and again reveals that the new scheme is accurate and convergent at all times.

Problem 4: Constant Coefficients CDR Model. In this example we simulate a linear convection-diffusion model presented in [27], see also [24]. The problem has coefficients, β_c and α_c:

$$\frac{\partial u}{\partial t} = \beta_c\frac{\partial u}{\partial x} + \alpha_c\frac{\partial^2 u}{\partial x^2},$$

where $\beta_c = 0.25; \alpha_c = 2500/\beta_c$. The exact solution is:

$$u(x,t) = \frac{1}{\sqrt{1+t}}e^{-\frac{(x-(1+t)\beta_c)^2}{4\alpha_c(1+t)}}.$$

The initial and boundary conditions are the exact solution evaluated at $t = 0$ and $x = \{0, 1\}$ respectively.

This problem is simulated with the presented schemes. The results obtained with different meshes and outputted after $t = 0.1$ and $t = 1.0$ are tabulated in Table 4. We can also see that these results confirm the theoretical results. Figure 4 displays the graphical results at different time steps. It can be seen that the computed numerical solution remains accurate even as time gets large. This, again, verifies the convergence of our method.

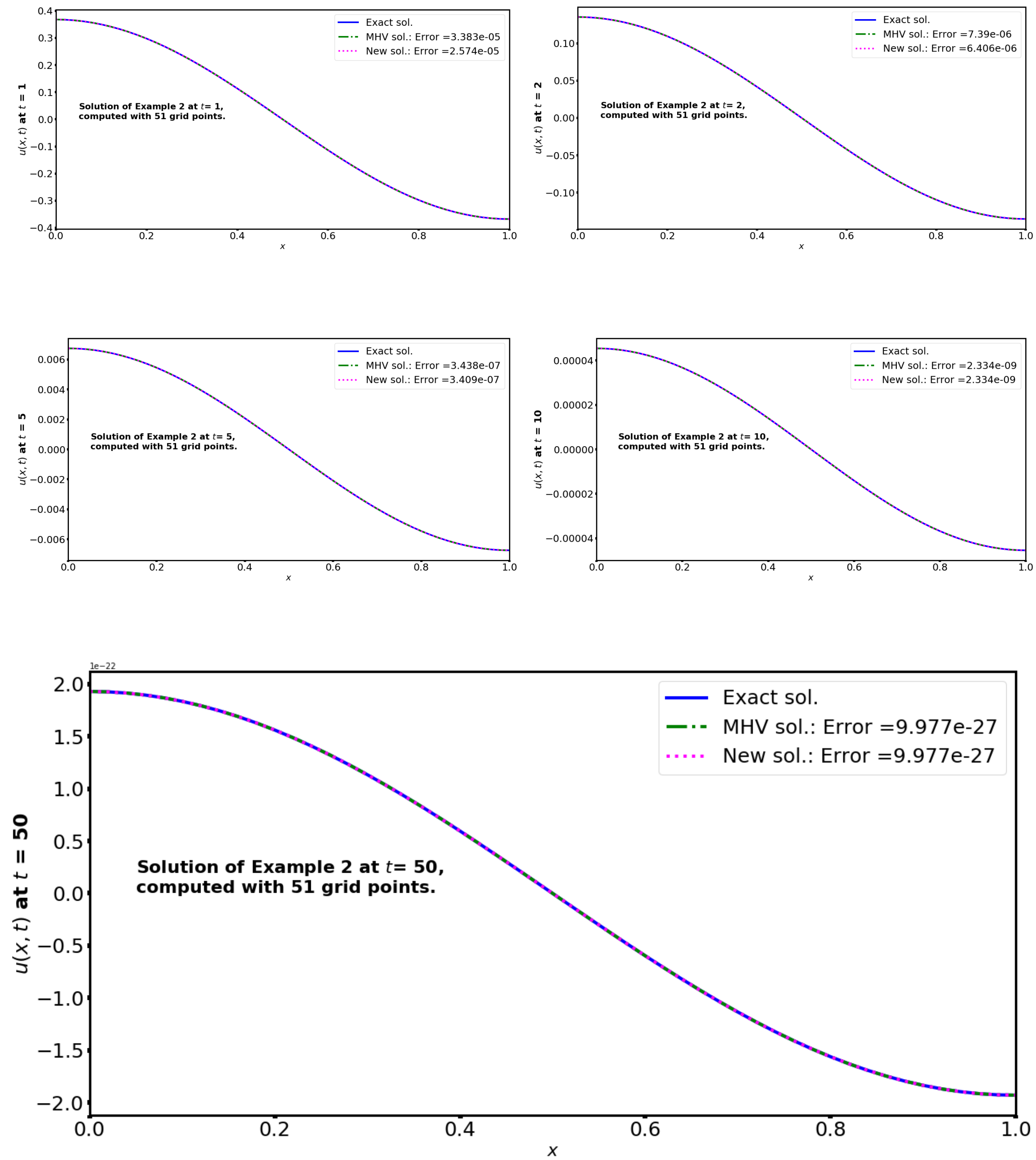

FIGURE 2. Exact and Numerical Solutions of Example 2 computed at different times on a grid of 51 points

Problem 5: Purely Convection - Linear Transport Model. Next, we apply the proposed method to the linear transport model (no diffusion - zero β) with the following coefficients:

$$q = -5; \beta = 0, f = s = 0.$$

TABLE 3. Numerical Results for Problem 3

M	MHV-Error	MHV-EOC	New Scheme-Error	New-Scheme-EOC
Results Outputted after time = 0.1				
4	0.0322024	-	0.0304921	-
8	0.0081321	1.98547	0.0074976	2.02394
16	0.00209222	1.95859	0.00188235	1.99389
32	0.000523248	1.99947	0.000470158	2.00132
64	0.000130935	1.99865	0.000117546	1.99992
128	3.27227e-05	2.00048	2.93851e-05	2.00007
Results Outputted after time = 1.0				
4	0.0123439	2.89012	0.0101775	2.84277
8	0.00270408	2.19059	0.00226207	2.16968
16	0.00065543	2.04462	0.000550117	2.03983
32	0.000162599	2.01113	0.000136595	2.00984
64	4.05698e-05	2.00284	3.40907e-05	2.00245
128	1.01372e-05	2.00074	8.51904e-06	2.00061

TABLE 4. Numerical Results for Problem 4

M	MHV-Error	MHV-EOC	New Scheme-Error	New-Scheme-EOC
Results Outputted after time = 0.1				
4	8.74254e-08	-	8.74266e-08	-
8	2.15025e-08	2.02355	2.15028e-08	2.02355
16	5.28114e-09	2.02558	5.2812e-09	2.02559
32	1.31883e-09	2.00159	1.31884e-09	2.00159
64	3.2935e-10	2.00156	3.29343e-10	2.00161
128	8.26185e-11	1.99508	8.23664e-11	1.99946
Results Outputted after time = 1.0				
4	1.91239e-08	-	1.91242e-08	-
8	4.74279e-09	2.01157	4.74284e-09	2.01157
16	1.18294e-09	2.00337	1.18295e-09	2.00337
32	2.95556e-10	2.00087	2.95558e-10	2.00087
64	7.388e-11	2.00017	7.3881e-11	2.00016
128	1.86713e-11	1.98436	1.8477e-11	1.99947

These coefficients reduce equation (1.1) to the linear transport model which is a hyperbolic problem:

$$\frac{\partial u}{\partial t} + 5\frac{\partial u}{\partial x} = 0,$$
$$u(x,0) = \sin(x), \quad u(0,t) = \sin(-5t).$$

The exact solution is:

$$u(x,t) = \sin(x - 5t).$$

This problem cannot be solved by MHV solver because the diffusion coefficient β is zero and the MHV solver involves a division by β. The example demonstrates the strength of the proposed scheme over the MHV solver. We simulate this problem by using the initial and boundary conditions derived from the exact solution. The results outputted after $t = 0.1$ and $t = 1.0$ are presented in Table 5. We can see that the new method performs very well, while the existing method (MHV) could not even attempt it.

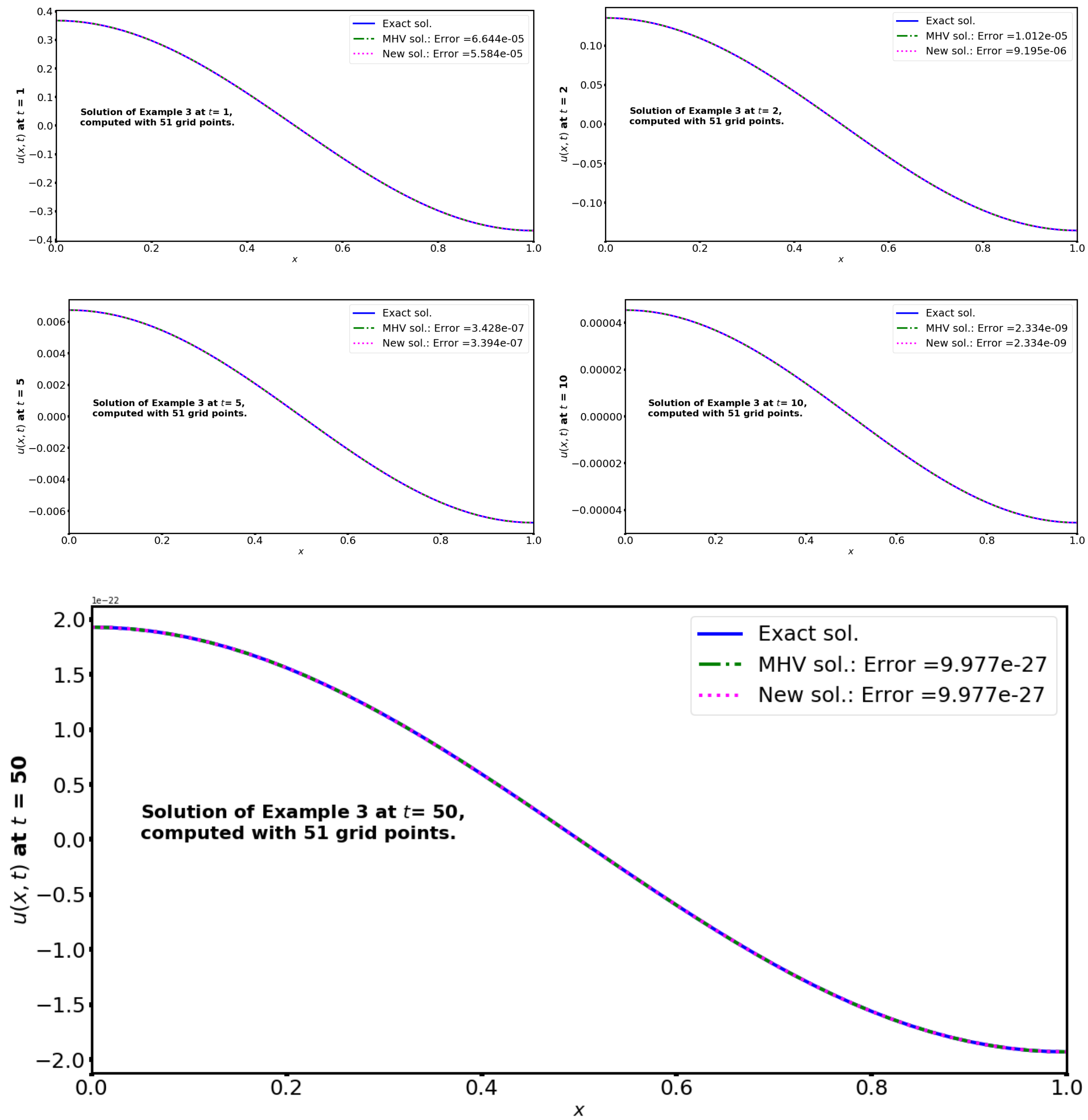

FIGURE 3. Exact and Numerical Solutions of Example 3 computed at different times on a grid of 51 points

This proves the efficacy of the new method for linear hyperbolic conservation laws, especially when the initial data is smooth. Again, these results are re-confirmed in Figure 5 where the solutions are plotted at different times. It is obvious that the numerical solution remains accurate even for large t. This is novel - the ability to be extremely competitive in both convection-diffusion problems ($\beta > 0$) and pure convection problems ($\beta = 0$).

Problem 6: Purely Convection - Burger's Equation with Nonlinear Source Term. Lastly, we investigate the method for fully nonlinear convection (inviscid Burger's) problem with complicated source (reaction)

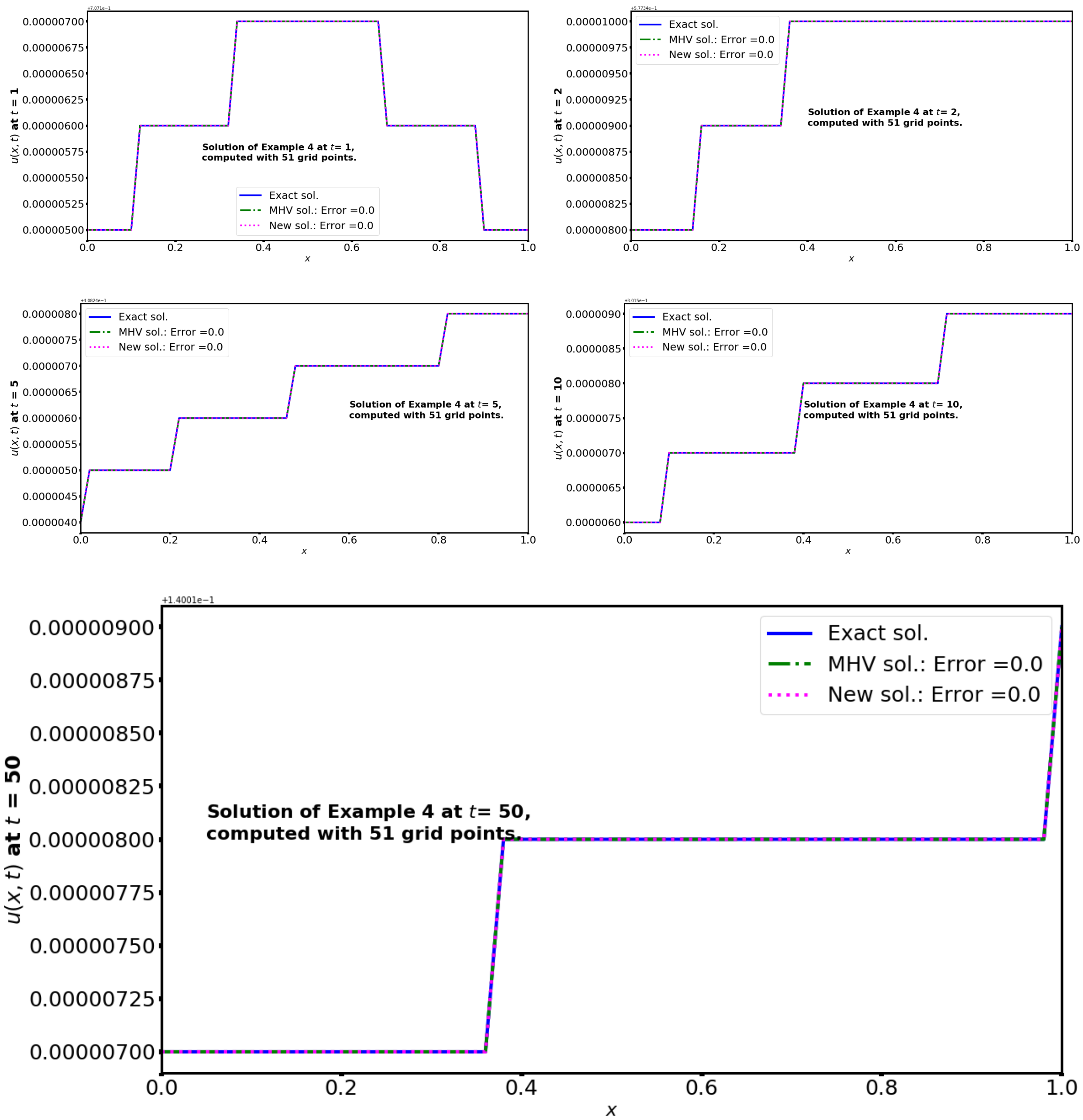

FIGURE 4. Exact and Numerical Solutions of Example 4 computed at different times on a grid of 51 points

terms.

$$\frac{\partial u}{\partial t} = q\frac{\partial u}{\partial x} + s(u, x, t) + f(u, x, t),$$

where the coefficients are

$$q(u, x, t) = u, \quad s(u, x, t) = -u^2 \sin(x + 5t),$$
$$f(x, t) = \big((\cos(x + 5t) + 1)^2 - \cos(x + 5t) - 6\big) \sin(x + 5t).$$

TABLE 5. Numerical Results for Problem 5

M	MHV-Error	MHV-EOC	New Scheme-Error	New-Scheme-EOC
Results Outputted after time = 0.1				
4	-	-	0.00572139	-
8	-	-	0.00117702	2.28123
16	-	-	0.000261745	2.16891
32	-	-	5.96671e-05	2.13315
64	-	-	1.42363e-05	2.06736
128	-	-	3.46995e-06	2.03659
Results Outputted after time = 1.0				
4	-	-	0.0150466	-
8	-	-	0.0029232	2.36381
16	-	-	0.000693321	2.07595
32	-	-	0.00016101	2.10638
64	-	-	3.83778e-05	2.0688
128	-	-	9.34257e-06	2.03838

The exact solution to the problem is:

$$u(x,t) = 1 + \cos(x + 5t).$$

The initial and boundary conditions are also obtained from the exact solutions. Four simulations are conducted with output times of $t = 1, 50, 100, 150$ and each repeated for different meshes (as in the previous test cases). The complete results are shown in Table 6. We can see that, even though this problem is hyperbolic, the numerical solution computed with our method agrees with the exact solutions. Again, we can see that for simulations with very short duration, the numerical results computed in very coarse grids are still very accurate. And the observation is that the shorter the duration of the simulation, the more accurate are results on coarse grids.

Another key observation is that even for long-duration simulations, accurate results can be obtained by refining the mesh, and this is beneficial since we do not have to modify the scheme - which is also easy to implement. Finally, Figure 6 shows the plots of the solution at different times. The fact that this example is nonlinear and hyperbolic means that it may lead to oscillatory solutions when computed with high order finite difference schemes on a very coarse grid. Here, a relatively coarse grid of 201 points is used to eliminate any form of oscillatory phenomenon as seen in Figure 6(e). Just like in the previous examples, this shows the ability of the new scheme to retain its second order spatial accuracy without oscillations for nonlinear hyperbolic problems. To the best of our knowledge, this is the first work that provides a scheme with these capabilities - able to retain second order accuracy for nonlinear hyperbolic (pure convection) problems, yet retains all the good features when used for convection-diffusion problem.

4.0.1. *Example 7.* This last case is adopted from example 2 in [11].

$$\frac{\partial u}{\partial t} = \frac{\partial}{\partial x}\left(\alpha(u)\frac{\partial u}{\partial x}\right) + \beta(u)\frac{\partial u}{\partial x} + f(x,t), \qquad x \in (-\pi, \pi), \quad t \in (0, 0.50),$$

$$u(-\pi, t) = u(\pi, t) = 0, \quad u(x, 0) = sin(2x),$$

where $\alpha(u) = u^2 + 1, \beta(u) = \sqrt{u+4}$ and

$$f(x,t) = \Big(-2\sqrt{e^t \sin(2x) + 4}\cos(2x) + 4e^{2t}\sin^3(2x) - 8e^{2t}\sin(2x)\cos^2(2x) + 5\sin(2x)\Big)e^t.$$

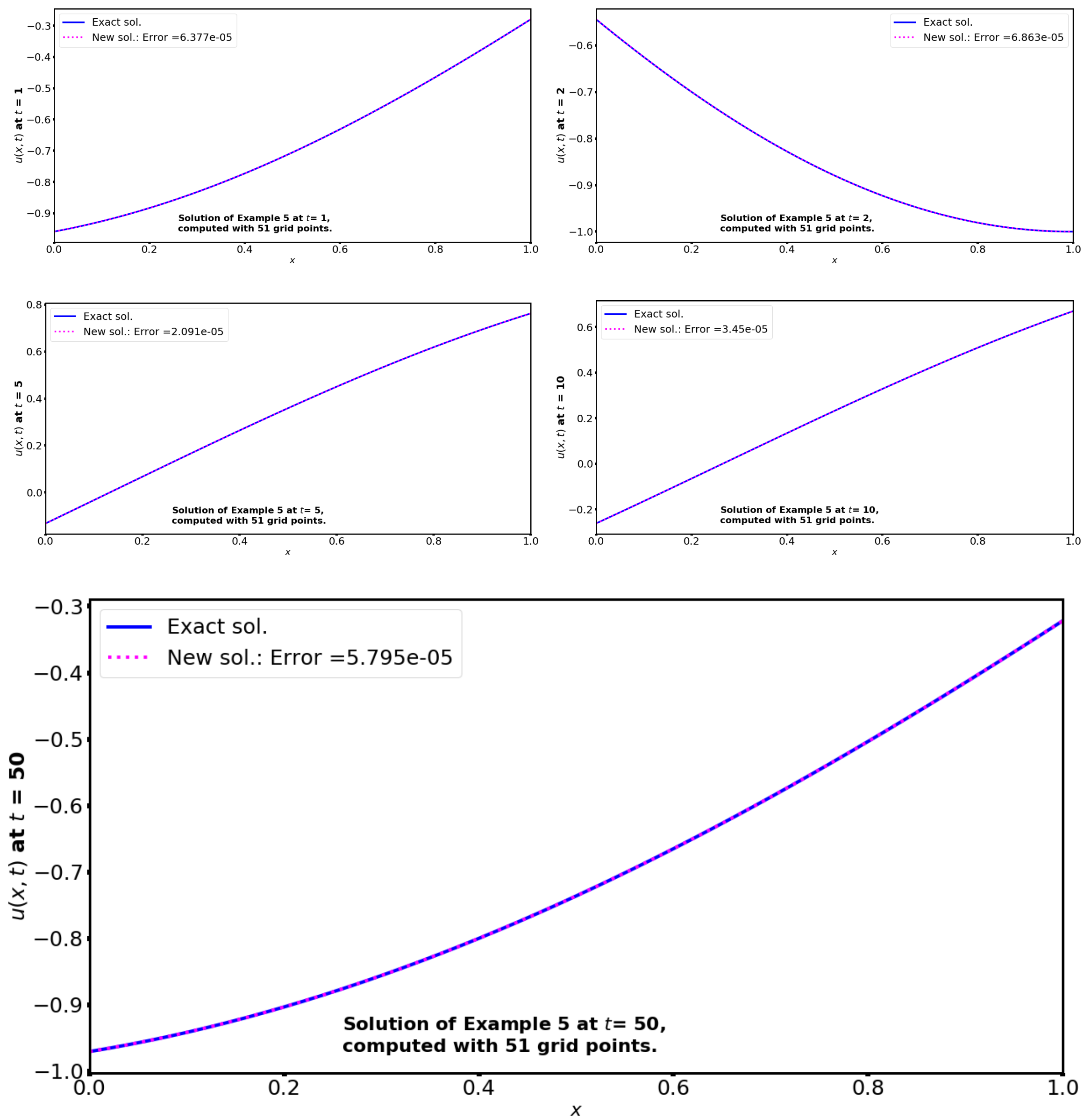

FIGURE 5. Exact and Numerical Solutions of Example 5 computed at different times on a grid of 51 points

The exact solution of this problem is $u(x,t) = e^t sin(2x)$, see [11]. The results of solving this problem using the two methods on several grid resolutions are reported. For further scrutiny, we have also included the results reported in [11] which involve four grid resolutions. These are shown in Table 7. It can be seen that the results of the three methods are comparable. Although the MHV scheme and that of [11] are slightly more accurate at very coarse grids, the EOCs indicate that the newly proposed scheme has really faster order of accuracy (see the EOCs), especially at the mesh gets finer. However, the strength of our newly proposed method is that apart from having a very competitive accuracy, it

TABLE 6. Numerical Results for Problem 6 outputted after different times

M	MHV-Error	MHV-EOC	New Scheme-Error	New-Scheme-EOC
Results Outputted after time = 1				
2	-	-	0.227112	-
4	-	-	0.0604762	1.90896
8	-	-	0.0195407	1.62988
16	-	-	0.00630346	1.63227
32	-	-	0.00179372	1.81319
64	-	-	0.000471705	1.927
128	-	-	0.000120209	1.97234
256	-	-	3.0269e-05	1.98963
Results Outputted after time = 50				
8	-	-	0.298605	-
16	-	-	0.0777101	1.94206
32	-	-	0.0241293	1.68732
64	-	-	0.00648362	1.89591
128	-	-	0.00156143	2.05393
Results Outputted after time = 100				
16	-	-	0.115965	-
32	-	-	0.0322942	1.84434
64	-	-	0.00763748	2.08011
128	-	-	0.00194269	1.97504
Results Outputted after time = 150				
16	-	-	0.0895622	-
32	-	-	0.045098	0.989826
64	-	-	0.0114367	1.97939
128	-	-	0.00300621	1.92765

can also be used when diffusion is zero, unlike the other schemes which would break down in such case.

TABLE 7. Numerical Results for Problem 7 outputted after different times. NA indicates not available data

N	Scheme [11]-Error	[11]-EOC	MHV-Error	MHV-EOC	New Scheme-Error	New-Scheme-EOC
20	0.185965	-	0.186118	-	0.216594	-
40	0.0527086	1.819	0.0527616	1.81866	0.0574482	1.91466
80	0.0136802	1.946	0.0136948	1.94586	0.0145356	1.98267
160	0.00345762	1.984	0.00346136	1.98421	0.00364198	1.9968
320	NA	NA	0.000867664	1.99613	0.000910487	2.00001
640	NA	NA	0.000217041	1.99917	0.000227556	2.00041
1280	NA	NA	5.42653e-05	1.99987	5.68769e-05	2.00031

4.0.2. *More Numerical Experiments.* We include more results to demonstrate (i) the first order time accuracy of our proposed scheme, and (ii)the performance of the scheme when β is small.

Table 8 shows the results of reducing the time step while repeatedly computing the solution of examples 1-3. It can be seen that the order of convergence (the third column) is one as theoretically proved in the analysis section. The result is the same for all three examples presented here.

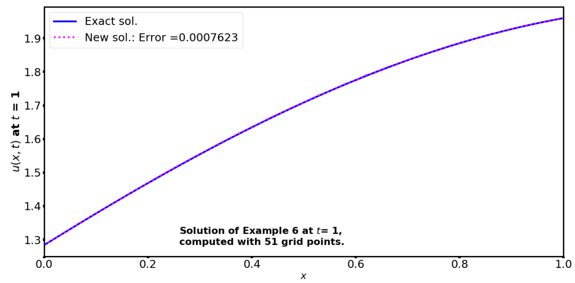

(a) Computed on a 51-point grid

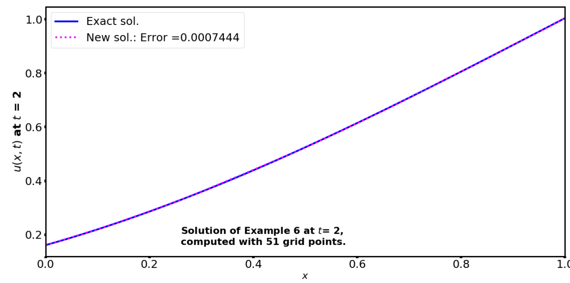

(b) Computed on a 51-point grid

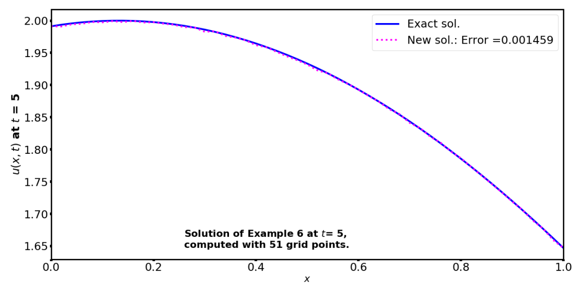

(c) Computed on a 51-point grid

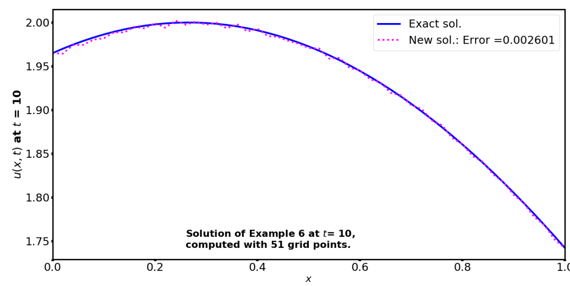

(d) Computed on a 51-point grid

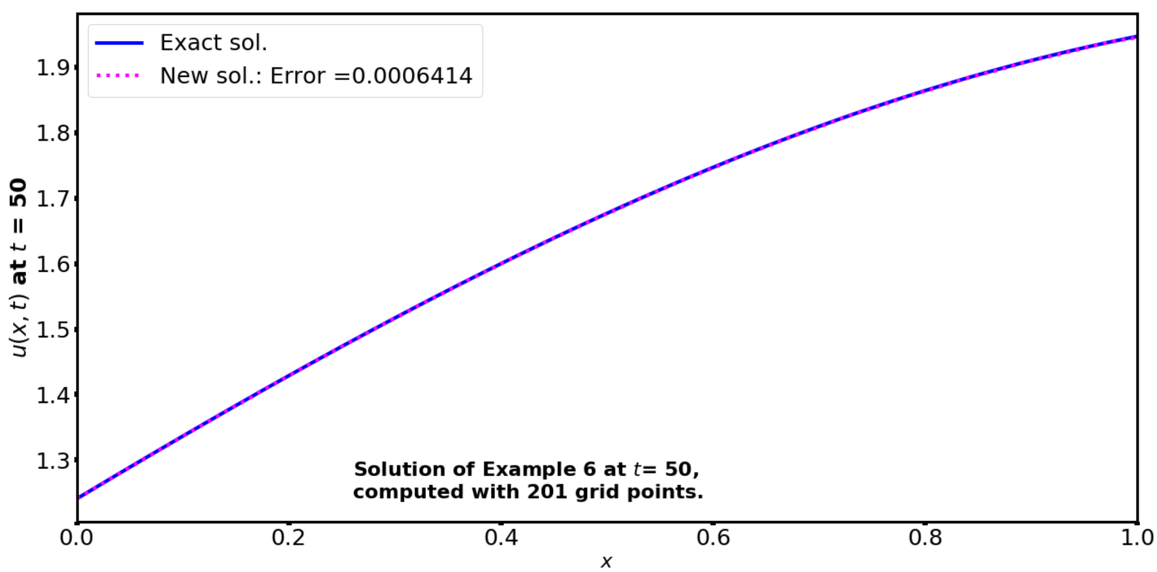

(e) Computed on a 201-point grid

FIGURE 6. Exact and Numerical Solutions of Example 6 computed at different times on a grid of 51 points (subfigures 6(a)-6(d)) and 201 points (subfigure 6(e))

Figure 7 shows the results computed for small $\beta = 10^{-7}$. These results are obtained by computing the solution of example 4 with this value of β. Figure 7 shows that the proposed scheme is very competitive. Although, we also observed that both the new method and the MHV scheme experience difficulties when β is much more smaller. This is quiet expected since the exact solution develops some form of boundary layer and these methods are not equiped with enough mechanisms to handle such cases. But in all, the results show that the new method is very promising.

Table 8. Experimental Order of Convergence with Respect to Time for Examples 1 to 3. These results verify the first order accuracy, with respect to time, of the method.

Δt	New Scheme-Error	New-Scheme-EOC
Results for Example 1 Outputted after time = 1		
0.1	0.603215	-
0.05	0.371383	0.699764
0.025	0.183489	1.01722
0.0125	0.0876827	1.06533
0.00625	0.0423848	1.04875
Results for Example 2 Outputted after time = 1		
0.1	0.000552507	-
0.05	0.000262002	1.07642
0.025	0.00012803	1.03309
0.0125	6.3571e-05	1.01004
0.00625	3.1951e-05	0.992511
Results for Example 3 Outputted after time = 1		
0.1	0.00587036	-
0.05	0.00283341	1.05091
0.025	0.00138835	1.02916
0.0125	0.000685436	1.01828
0.00625	0.000338975	1.01584

5. Conclusion

A new numerical scheme has been proposed and analyzed for convection-diffusion-reaction equations with nonlinear coefficients. The boundedness of the computed solution is established by deriving the lower and upper bounds. Consistency is also proved in maximum norm. In addition to high accuracy and compactness, the scheme is able to simulate purely convection problems, at least over short times when shocks do not appear; which is an advantage over some existing methods. Examples are provided to demonstrate all these claims. It is recommended that the proposed scheme should be selected over the MHV solver, especially for CDREs problems in which convection dominates diffusion, or diffusion is likely to vanish. A further study is recommended in the direction of extension to multi-dimensions.

References

[1] E. Audusse, F. Bouchut, M.O. Bristeau, R. Klein, and B. Perthame, *A fast and stable well-balanced scheme with hydrostatic reconstruction for shallow water flows*, SIAM Journal Scientific Computing **25** (2004), 2050–2065.

[2] D. S. Balsara, S. Garain, and C.-W.Shu, *An efficient class of weno schemes with adaptive order*, Journal of Computational Physics **326** (2016), 780–804.

[3] F. Baronio, A. Chabchoub, G. Esler, J. Field, J. Gaskell, I. Hewitt, S. Lombardo, S. Marquis, C. Nwaigwe, A. Tzella, et al., *Hydraulic modelling of collection networks study group 2: Maths foresees project report*, (2018).

[4] L. Bers, F. John, and M. Schechter, *Partial Differential Equations*, American Mathematical Society, 1964.

[5] H. P. Bhatt and A.-Q. M. Khaliq, *Fourth-order compact schemes for the numerical simulation of coupled burgers' equation*, Computer Physics Communications **200** (2016), 117–138.

[6] J. Chen and Y. Ge, *High order locally one-dimensional methods for solving two-dimensional parabolic equations*, Advances in Difference Equations **2018**(2018): 361. https://doi.org/10.1186/s13662-018-1825-2.

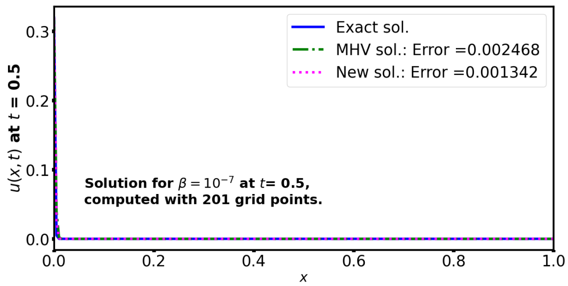

(a) Solution at $t = 0.5$

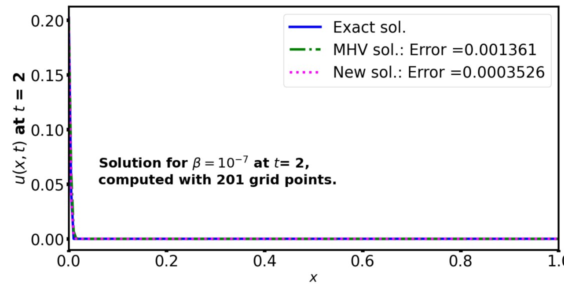

(b) Solution at $t = 1$

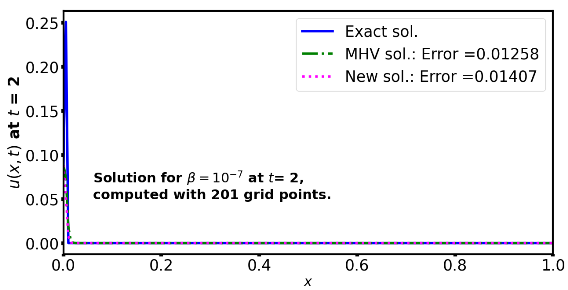

(c) Solution at $t = 2$

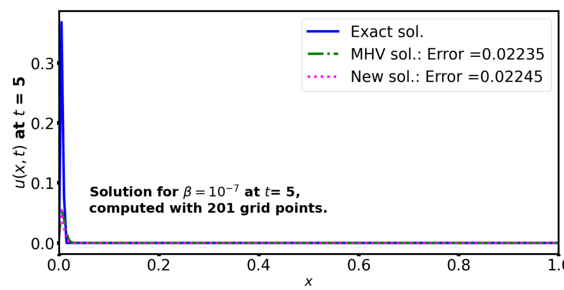

(d) Solution at $t = 5$

FIGURE 7. Solutions computed for small $\beta = 10^{-7}$ at different times

[7] E. Dremkova and M. Ehrhardt, *A high-order compact method for nonlinear black–scholes option pricing equations of american options*, International Journal of Computer Mathematics **88** (2011), no. 13, 2782–2797.

[8] G. Guennebaud, B. Jacob, et al., *Eigen v3*, http://eigen.tuxfamily.org, 2010.

[9] G. Gurarslan, H. Karahan, D. Alkaya, M. Sari, and M. Yasar, *Numerical solution of advection-diffusion equation using a sixth-order compact finite difference method*, Mathematical Problems in Engineering **2013** (2013): 672936 http://dx.doi.org/10.1155/2013/672936.

[10] T. T. H. Hanh, D. N. H. Thanh, et al., *Monotone finite-difference schemes with second order approximation based on regularization approach for the dirichlet boundary problem of the gamma equation*, IEEE Access **8** (2020), 45119–45132.

[11] L. M. Hieu, T. T. H. Hanh, and D. N. H. Thanh, *A finite-difference scheme for initial boundary value problem of the gamma equation in the pricing of financial derivatives*, Journal of Mathematics and Computer Science **20** (2020), no. 4, 283–291.

[12] W. Hundsdorfer and J. G. Verwer, *Numerical Solution of Time-Dependent Advection-Diffusion-Reaction Equations*, Springer Science and Business Media, 2013.

[13] G.D. Hutomo, J. Kusuma, A. Ribal, A. G. Mahie, and N. Aris, *Numerical solution of 2-d advection-diffusion equation with variable coefficient using du-fort frankel method*, Journal of Physics: Conference Series, vol. 1180, IOP Publishing, 2019, p. 012009.

[14] O. Hyong-Chol, J.-J. Jo, and J.-S. Kim, *General properties of solutions to inhomogeneous black–scholes equations with discontinuous maturity payoffs*, Journal of Differential Equations **260** (2016), no. 4, 3151–3172.

[15] D. Kuzmin, *A guide to numerical methods for transport equations*, University Erlangen-Nuremberg (2010), 24.

[16] M. H. Le, T. H. H. Truong, and N. H.T. Dang, *Finite-difference scheme for initial boundary value problems in financial mathematics*, VNU Journal of Science: Mathematics-Physics **35** (2019), no. 4, 79-86.

[17] V. Lefèvre, A. Garnica, and O. Lopez-Pamies, *A weno finite-difference scheme for a new class of hamilton–jacobi equations in nonlinear solid mechanics*, Computer Methods in Applied Mechanics and Engineering **349** (2019), 17–44.

[18] R. J. Leveque, *Numerical Methods For Conservation Laws.*, Birkhäuser Verlag, 1992.

[19] ______, *Finite Volume Methods For Hyperbolic Problems*, vol. 31, Cambridge University Press, 2002.

[20] P. Matus, *On convergence of difference schemes for ibvp for quasilinear parabolic equations with generalized solutions*, Computational Methods in Applied Mathematics **14** (2014), no. 3, 361–371.

[21] P. Matus, F. Gaspar, V. T. Kim Tuyen, et al., *Monotone difference schemes for weakly coupled elliptic and parabolic systems*, Computational Methods in Applied Mathematics **17** (2017), no. 2, 287–298.

[22] P. Matus, L. G. Vulkov, et al., *Analysis of second order difference schemes on non-uniform grids for quasilinear parabolic equations*, Journal of Computational and Applied Mathematics **310** (2017), 186–199.

[23] P. P. Matus and D. B. Poliakov, *Consistent two-sided estimates for the solutions of quasilinear parabolic equations and their approximations*, Differential Equations **53** (2017), no. 7, 964–973.

[24] A. Mohebbi and M. Dehghan, *High-order compact solution of the one-dimensional heat and advection–diffusion equations*, Applied Mathematical Modelling **34** (2010), 3071–3084.

[25] K. W. Morton and D. F. Mayers, *Numerical Solution of Partial Differential Equations: an introduction*, Cambridge University Press, 2005.

[26] S. Mungkasi, *A Study of Well-Balanced Finite Volume Methods And Refinement Indicators For The Shallow Water Equations*, Ph.D. thesis, The Australian National University, 2012.

[27] B. J. Noye, *A new third-order finite-difference method for transient one-dimensional advection—diffusion*, Communications in applied numerical methods **6** (1990), no. 4, 279–288.

[28] C. Nwaigwe, *Mathematical modelling of ground temperature with suction velocity and radiation*, American Journal of Scientific and Industrial Research **1** (2010), no. 2, 238–241.

[29] C. Nwaigwe, *Coupling Methods for 2d/1d Shallow Water Flow Models for Flood Simulations*, Ph.D. thesis, University of Warwick, United Kingdom, 2016.

[30] C. Nwaigwe, *Analysis and application of a convergent difference scheme to nonlinear transport in a brinkman flow*, International Journal of Numerical Methods for Heat & Fluid Flow **30**(2020), no. 10, 4453-4473.

[31] ———, *Sequential implicit numerical scheme for pollutant and heat transport in a plane-poiseuille flow*, Journal of Applied and Computational Mechanics **6** (2020), no. 1, 13–25.

[32] ———, *Mathematical modeling and numerical analyses of transport phenomena with variable cross-diffusion and nonlinear radiation*, Computational Thermal Sciences: An International Journal **13** (2021), no. 1, 73-96.

[33] C. Nwaigwe and O. D. Makinde, *Finite difference investigation of a polluted non-isothermal non-newtonian porous media flow*, Diffusion Foundation **26** (2020), 145-156.

[34] A. A. Samarskii, *The Theory of Difference Schemes*, New York: Marcel Dekker, 2001.

[35] C. Shen, J. M. Qiu, and A. Christlieb, *Adaptive mesh refinement based on high order finite difference weno scheme for multi-scale simulations*, Journal of Computational Physics **230** (2011), no. 10, 3780–3802.

[36] C.-W. Shu, *High order weighted essentially nonoscillatory schemes for convection dominated problems*, SIAM Review **51** (2009), no. 1, 82–126.

[37] ———, *High order weno and dg methods for time-dependent convection-dominated pdes: A brief survey of several recent developments*, Journal of Computational Physics **316** (2016), 598–613.

[38] E. F. Toro, *Riemann Solvers and Numerical Methods for Fluid Dynamics: A Practical Introduction*, Springer Science & Business Media, 1999.

[39] ———, *Shock Capturing Methods For Free-Surface Flows*, Wiley, 2001.

[40] A. Weli and C. Nwaigwe, *Numerical analyses of channel flow with velocity-dependent suction and nonlinear heat source*, Journal of Interdisciplinary Mathematics **23** (2020), no. 5, 987-1008.

[41] Z. Wu, *Nonlinear Diffusion Equations*, World Scientific, 2001.

[42] X. Zhong and C.-W. Shu, *A simple weighted essentially nonoscillatory limiter for runge–kutta discontinuous galerkin methods*, Journal of Computational Physics **232** (2013), no. 1, 397–415.

[43] J. Zhu, J. Qiu, and C.-W. Shu, *High-order runge-kutta discontinuous galerkin methods with a new type of multi-resolution weno limiters*, Journal of Computational Physics **404** (2020): 109105.

Institute for Ground Water Studies, University of the Free State, Bloemfontein, South Africa; and Department of Mathematics, Rivers State University, Port Harcourt, Nigeria

Current address: Bloemfontein, South Africa

Email address: `nwaigwe.chinedu@ust.edu.ng`